Electrostatic forces acting on the tip in atomic force microscopy: Modelization and comparison with analytic expressions

S. Belaidi,[a] P. Girard, and G. Leveque
Laboratoire d' Analyse des Interfaces et de Nanophysique, UPRESA CNRS 5011, Case courrier 82, Place Eugène Bataillon, 34095 Montpellier cedex 5, France

(Received 25 April 1996; accepted for publication 18 October 1996)

With the model of equivalent charge distribution, we calculated the exact electrostatic force acting on the real (conical) tip of an atomic force microscope. This model applies to a conductive tip in front of a conductive plane. We compared the equivalent charge model with several analytic models used to date to approximate the electrostatic forces and discussed their degree of validity. We estimated the contribution of the cantilever to the total force and showed, on the basis of theoretical calculations and experimental results, that the contribution of cantilever may constitute the essential part of the electrostatic force in the range of distances used in electrostatic force microscopy in the air. © *1997 American Institute of Physics.* [S0021-8979(97)00803-7]

I. INTRODUCTION

Resulting from the scanning tunneling microscope,[1] the atomic force microscope (AFM) is a powerful tool for imaging and studying the surfaces of objects. For this kind of microscope, a sharp tip mounted on a cantilever is applied to the sample, and the topography of the object is imaged by detecting the cantilever bending. Usually, the microscopes are provided with a servo-control which allows the tip to scan the surface with a constant deflection (contact mode), or with a constant amplitude of vibration (non-contact mode).[2]

In contact mode, the Van der Waals repulsion force sets the tip-sample distance at a few angströms, which allows us to obtain images that give the atomic periodicity.[3,4] In non-contact mode, the probe detects the Van der Waals attractive forces,[5] magnetic,[6] or electrostatic forces[7–12] which allows us to obtain other information than purely topographical. If a voltage is applied between the object and the tip of microscope (both of them conductive), an attractive force is added and the electrostatic force and its local variations can be imaged by the microscope. We then talk about an electrostatic force microscope (EFM). The interest in this new microscopy is its ability to image the local voltages of working microelectronic structures[8,13] and to measure local electrostatic fields[14] or charges on insulator surfaces.[15]

The images obtained by EFM are strongly dependent on the shape and dimensions of the tip as well as the type of sample. One of the main difficulties in analyzing images lies in the lack of simple analytic models to describe the force acting on the tip of microscope in the environment of a polarized object. This comes from the fact that the electrostatic sensor has a complex shape: a cantilever hold a conical or pyramidal tip ending in a spherical apex.

Thus, in the literature, several models based on analytic expressions are used to determine the electrostatic force: the sphere model,[16] the uniformly charged line model,[17] the knife edge model.[18] These different models are coherent with the experimental results in restricted ranges of distances. Electrostatic force has also been investigated by numerical simulations such as finite differences[19] and the surface charge method.[20]

Below we propose to give a more convenient expression of the electrostatic force between a tip and a metallic plane taking into account the real shape of the available tips and cantilevers. This approach allows us to determine the limits of the classical approximations, and to recommend conditions under which electrostatic microscope can be used. In Sec. II, we apply equivalent charge model which produces the same equipotentials and forces as those between the tip and the surface plane. Then, we compare these results with several analytic models used to approximate electrostatic forces. In Sec. III, we take into account the presence of the cantilever in the equivalent charge model in order to evaluate its contribution to the total force. Finally, in Sec. IV, using theorical calculations and experimental results, we discuss the importance of the different parts of the electrostatic sensor in standard EFM conditions of operation.

II. MODELIZATION OF ELECTROSTATIC FORCES APPLIED TO A SINGLE TIP

After a description of the tip shapes, we examine the voltage distribution and electrostatic forces existing between two conductive elements: the tip and an infinite plane taken as the sample.

A. Shape of the tip

The tips used in AFM are of two different types, metallized tips of silicon nitride with half angle 35° or conical structures made of doped silicon with half angle 10°. The tip is fixed to a «V» shaped cantilever (Fig. 1), slightly inclined to the sample plane. These tips end with rounded surfaces of radius R (Fig. 2). The real shape of the tips, even new, fluctuates about nominal values and presents more or less observable defects. In order to simplify calculations, we deal with the following typical geometries:

(a) Cone of half angle 10° ending in an apex radius of the order of 10 nm, to represent real sharp silicon tips (tip A).

(b) Cone of half angle 35° to represent real silicon nitride tips with an apex radius of 50 nm to 100 nm depending

[a]Electronic mail: belaidi@lain.univ-montp2.fr

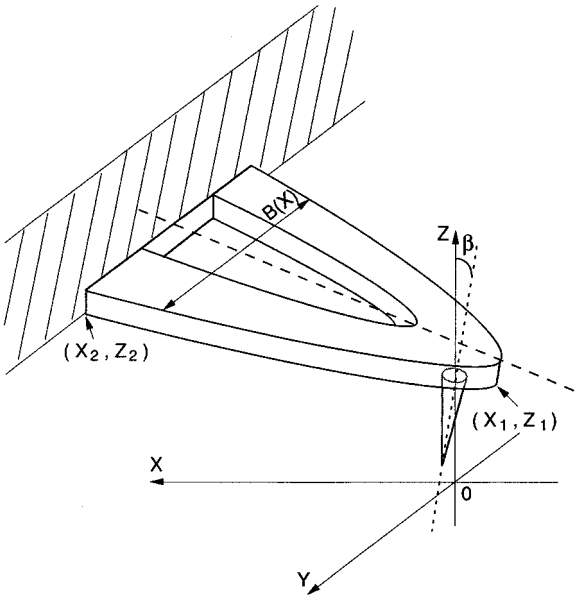

FIG. 1. Schematic drawing of a probe tip fixed to a cantilever in AFM.

on the metal coating (tip B). A silicon nitride tip with a pyramidal shape could be considered as a conical tip. In fact, the pyramidal shape gives forces which are intermediate between two cones: one included in the pyramid, the other includes the pyramid itself. Then, the cone angle difference does not exceed 10°. We shall see later [Fig. 5(a)] that the force does not depend drastically on the cone angle, so the conical approximation is suitable.

(c) Cone of variable angle (tip C) or length (tip D), in order to explore intermediate cases.

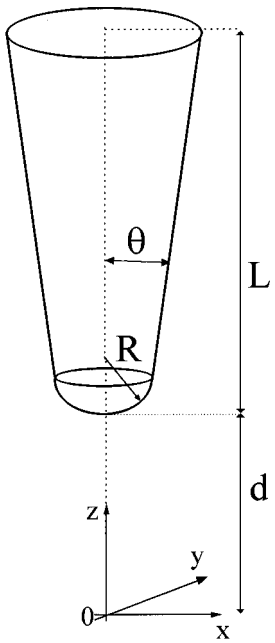

FIG. 2. Detailed representation of a tip with its geometrical characteristics.

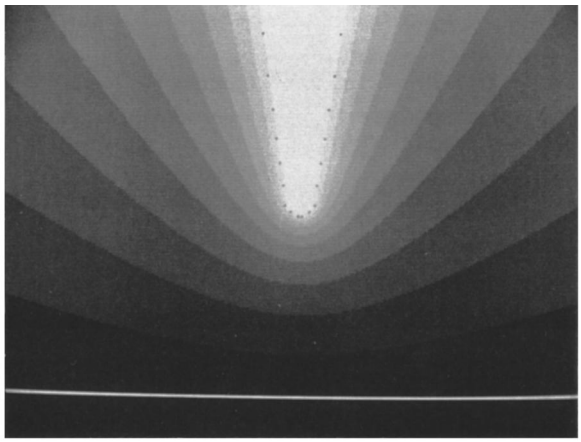

FIG. 3. Equipotentials obtained by the equivalent charge model for a tip A_1 ($L=4$ μm, $\theta=10°$, $R=10$ nm) at the potential $V_0=1$ V.

B. Potential distribution between a conical rounded tip and the plane

Our method is based on the principle of distribution of equivalent charges which enables us to replace a conductor in equilibrium with a set of fictive charges inside it, putting into practice the image method of equipotentials, it is the equivalent charge model (ECM) taking into account the revolution symmetry of the tip, a distribution of N charges on the z axis allows us to build an equipotential surface $V_0=1$ following exactly the shape of the tip (see Fig. 2). Since the force is proportional to V_0^2, the results can be extended to any tip-sample polarization. From a practical point of view, N charges set in $\mathbf{r}_i$ positions (on the z axis) must produce a potential V_0 at $\mathbf{r}_n$ positions of N points spread all over the tip surface. The method gives satisfactory results for the regular spreading of $\mathbf{r}_i$ and $\mathbf{r}_n$ points as in Fig. 3. The inclinations of the tip in real EFM (about 20°) does not significantly affect the results. This assumption shall be confirmed later. The conductive plane at a zero potential is created by the introduction of an electrostatic image tip with $-q_i$ charges at $-\mathbf{r}_i$ points. The q_i are then solutions to the following system:

$$\frac{1}{4\pi\epsilon_0}\sum_{i=1}^{N}\left(\frac{q_i}{|\mathbf{r}_n-\mathbf{r}_i|}-\frac{q_i}{|\mathbf{r}_n+\mathbf{r}_i|}\right)=V_0(\mathbf{r}_n) \tag{1}$$

for $n=1,2,\ldots,N$ and $V_0(\mathbf{r}_n)=V_0$.

C. Electrostatic force

With the above distribution of charges, we calculate the force acting on the tip in front of the conductive plane at zero potential, which is equal to the total force between the charges q_i of the tip and $-q_j$ of the image:

$$F_{\mathrm{p}}(d)=\frac{1}{4\pi\epsilon_0}\sum_{j=1}^{N}\sum_{i=1}^{N}\frac{-q_iq_j}{|\mathbf{r}_i+\mathbf{r}_j|^2}, \tag{2}$$

q_i and q_j are both dependent on the tip-sample distance.

The $F_{\mathrm{tip}}(d)$ values obtained for different types of tip are shown in Fig. 4. For distances lower than 1 nm, one model

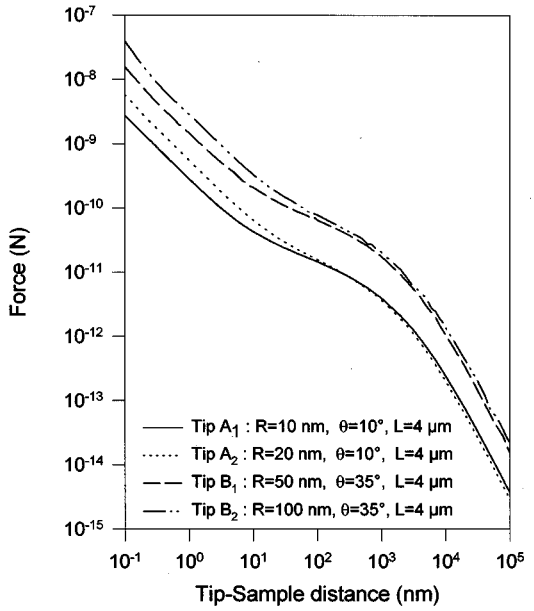

FIG. 4. Electrostatic force against tip-sample distance d for two types of tip: A and B, at the potential 1 V calculated by the equivalent charge model.

gives only an approximation of the force, since the atomic nature of the medium should be considered.

The $F_{\text{tip}}(d)$ is characterized by three distinct zones with different slopes. For small distances ($d<10$ nm), the linear shape of the $F_{\text{tip}}(d)$ function in logarithmic scale indicates an $F \propto 1/d$ dependence. In the opposite side ($d>10$ μm), the law is $F \propto 1/d^2$, as can be expected when the tip is far from the plane. The d dependence in the intermediate region (10 nm$<d<10$ μm) has a lower slope and will be discussed later. In this zone, the magnitude of the force increases with the cone aperture θ [Fig. 5(a)] and the cone length [Fig. 5(b)]. This observation indicates that the lateral surface of the tip may govern the total force in this range.

D. Comparison with analytic models

We now compare the force calculated for the real geometry of the tip with the forces obtained in simplified geometries. The details concerning the calculations of the electrostatic force for these geometries are given in the appendix. All results are reported in Fig. 6.

For small distances ($d \leqslant 10$ nm), three models: the single charge model, the knife edge and the sphere model, describe the behaviour of the tip in satisfactory way. However, the expression [(A7) in the Appendix] of the knife edge model needs a width l, which is not experimentally defined. The value of $l=50$ nm used in Fig. 6 has been chosen to fit the other curves, which means that the knife edge model needs an external parameter to be used. For small distances, the best model is definitely the sphere model, as it is based on the same spherical apex geometry as the real tip. The single charge model is also useful because of its simple expression, but gives errors in the force always greater than 25%.

Beyond 20 nm, the hyperboloid and the charged line models give convenient approximations of the real force. This agreement comes from the fact that both models reproduce the conical shape of the tip far from the apex. Discrepancies arise between these models and the exact value for large distances ($d>10$ μm), due to the fact that we have to introduce an artificial tip length in the hyperboloid and in the charged line models. Next, using the uniformly charged line model, we have found that a 20° inclination of the tip produces only a 10% increase of the force for distance $d=10$ nm. So, this effect of inclination may be neglected for distances of usual use in EFM. This confirms our initial assumption.

The simple model of the two flat surfaces is not convenient for small distances but can be used for the test if the tip apex is flat instead of spherical.

In the third range ($d>10$ μm), the distance d is larger than the tip length and the whole tip contributes to the electrostatic force. The force on a real conical tip can not be

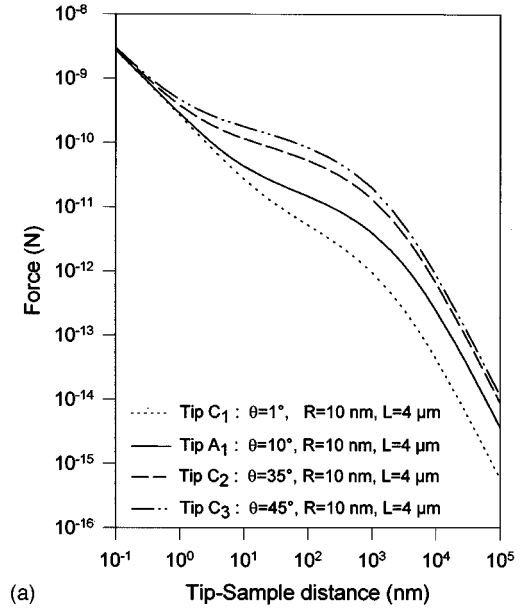

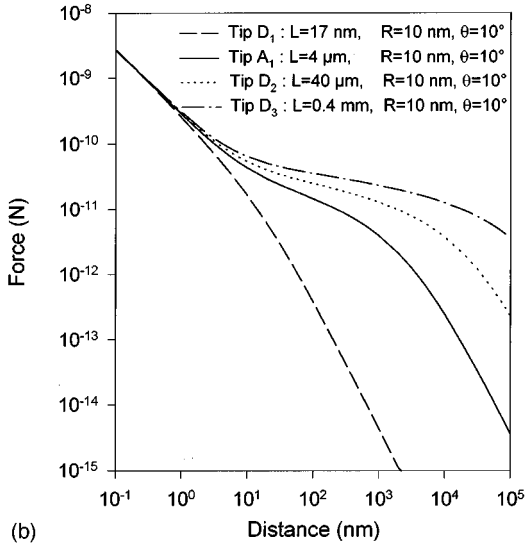

FIG. 5. Variation of the dependence of the force on the d tip-sample distance with modification of (a) the half angle θ, and (b) length L of the tip deduced from our model. We compare these curves with the tip A_1 used as the reference.

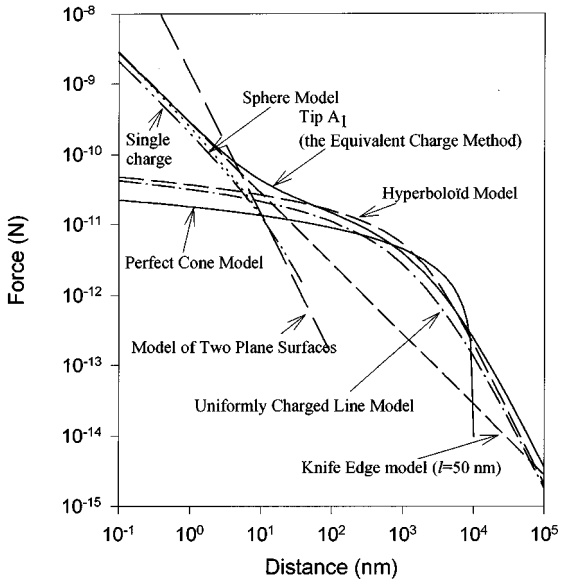

FIG. 6. Comparison of theoretical curves force against d distance obtained by the equivalent charge model for a tip A_1 with those deduced from simple analytic models. The voltage applied is always 1 V. — single tip A_1: $R=10$ nm, $\theta=10°$, $L=4$ μm, ----- the sphere model ($R=10$ nm), —- the uniformly charged line model (length $L=4$ μm, $\lambda=2.27\times10^{-11}$ C/m), —- the single charge model, –– the knife edge model ($l=50$ nm), — the perfect cone model ($\theta=10°$, $L=4$ μm), –– the hyperboloid model, ($rc=3$ μm) with asymptotical branches at 10°, — the model of two plane surfaces ($A=\pi R^2$).

deduced simply, but is certainly lower than that on the sphere of radius $L/2$ which encompasses the whole tip.

To summarize, we recommend the use of two approximate models for the tip-plane interaction: the spherical model for small and large distances (slightly modified in this last case) and the perfect cone model or uniformly charged line for intermediate distances. This leads to the d dependences shown in Table I. As the real $F_{\text{tip}}(d)$ curve in Fig. 6 is continuous from one range to another, the intermediate range is of variable length, and an apparent experimental dependence in $1/d^{05}$ can be obtained.[13] The above three ranges correspond to the case where the force is mainly localized on the tip apex, on the conical part of the tip, and on the tip as a whole when the distance is large. The limits of the three ranges can be estimated by making the expressions in Table I equal. Qualitatively, the first expression is convenient when the distance is much smaller than the radius of the apex, and the third when the distance is much larger than the length of the tip. The exact limits are dependent on angle θ but are not useful as a convenient $F(d)$ can be built by simply adding the three expressions in Table I.

TABLE I. Analytic expressions for the electrostatic force. $\lambda(\theta)$ is the charge density given in Eq. (A11). $s(\theta)=a\theta+b$ is an semi-empirical factor with values given in Eq. (A4).

	Very small tip-sample distance $d<R$	Intermediate distance $(R<d<L)$	Large tip-sample distance $d>L$
Model	Sphere	Uniformly charged line	Modified sphere
Expression of the force F	$\pi\epsilon_0 V_0^2 \frac{R}{d}$	$\frac{\lambda(\theta)^2}{4\pi\epsilon_0}\ln\left(\frac{L}{4d}\right)$	$\pi\epsilon_0 V_0^2\left(\frac{L}{2d}s(\theta)\right)^2$
Gradient $\frac{\partial F}{\partial d}$	$\propto\frac{1}{d^2}$	$\propto\frac{1}{d}$	$\propto\frac{1}{d^3}$
Localization of the force on the tip	Apex	Tip side	not localized

III. OTHER STATIC FORCES

Two attractive forces disturb the previous modelization. These are the Van der Waals forces between the tip and the plane, and the electrostatic force applied on the lever supporting the tip.

A. Van der Waals forces

In Hartmann's simplified model,[21] the Van der Waals attractive force is additive and can be calculated as an integral of the local pressure $p(z)$

$$F_{\text{VdW}}=2\pi\int_0^\infty zp[z(x)]dx$$

$$\text{with } z(x) \text{ the tip shape equation} \qquad (3)$$

where

$$p(z)=\frac{H_n}{6\pi z^3}\tanh\left(\frac{\lambda_{123}}{z}\right).$$

H_n is the Hamaker constant for a tip and a metallic plane, λ_{123} is a suitable constant. This expression takes into account the actual shape of the tip through the $z(x)$ function, and the delayed expression of VdW force with the $\tanh(\lambda_{123}/z)$ term. The intensity of this force shown in Fig. 7 is approximately a d^{-2} force for short distances ($d<\lambda_{123}$). Its amplitude is higher than the electrostatic force for $V_0=1$ at distances inferior to a few nanometers.

B. Electrostatic force on the cantilever

The expression of the force on the cantilever can be deduced approximately from the parallel plane capacitor one. To take into account the shape of the cantilever whose width and distance depend on x, we introduce the $B(x)$ function describing the width of the cantilever and $Z(x)$ its distance to the plane. The cantilever is inclined at angle β to the reference plane, and its distance to the plane depends on x in the following way: $Z(x)=L+d+x\tan\beta$. So, for the set up in Fig. 1, the force acting on the cantilever can be written as an integral:

$$F_{\text{cantilever}}=\frac{\epsilon_0 V^2}{2}\int_{x_1}^{x_2}\frac{B(x)dx}{Z(x)^2}, \qquad (4)$$

x_1 and x_2 are, respectively, the coordinates of the lower and upper end of the cantilever. We neglect the border effect of the capacitor and the thickness of the cantilever.

The function $F_{\text{cantilever}}(d)$ is shown in Fig. 7. Note that the force applied on the tip prevails for small distances (d

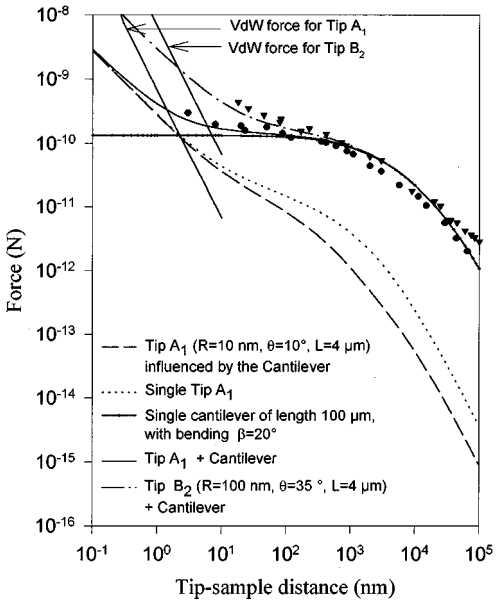

FIG. 7. Electrostatic force on the tip, the cantilever and the tip-Cantilever obtained by the equivalent charged model for tip A_1 and B_2 at the potential 1 V. Solid dots and solid triangles represent, respectively, the experimental data for the tip A_1 and the tip B_2 Van der Waals (VdW) forces are plotted for comparison.

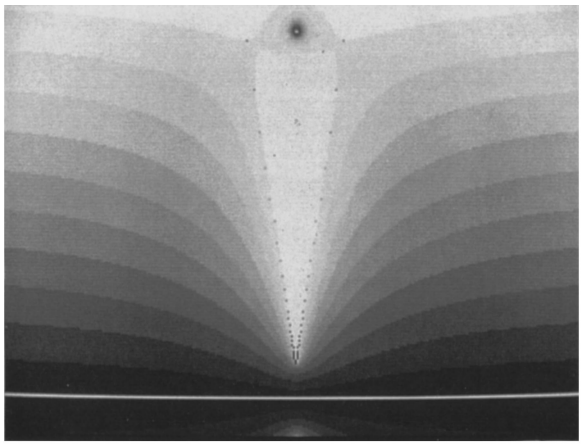

FIG. 8. Equipotentials obtained by the equivalent charge model for a tip A_1 ($L=4$ μm, $\theta=10°$, $R=10$ nm) with the cantilever (both at the potential $V_0=1$). The black dot at the upper part of the tip is due to the negative charge used to neutralize the cantilever charge density.

<10 nm for the A tips, $d<100$ nm for the B tips). For large distances, the cantilever gives the main contribution to the force.

C. Force applied on the tip-cantilever system

Theorically, the resulting force on the EFM sensor is not just the superposition of the two precedent forces (F_{tip} and $F_{\text{cantilever}}$) because the electrostatic interactions between the tip and the cantilever change the potential distribution. The complete system is more difficult to treat precisely because it brings together the force on the tip calculated by means of the equivalent charge model with a revolution symmetry, and the force on the cantilever for which this symmetry does not exist.

We therefore chose a mixed model for which the force acting on the tip is considered a local perturbation, with revolution symmetry, included in a nonsymmetric and larger system (cantilever=capacitor). The distribution of charges on the conductive system (cantilever+tip) can be split into superficial charges located on the lower plane of the cantilever plus charges located on the tip. As the presence of the tip disturbs the charge distribution on the cantilever and vice versa, we introduce two distributions in a rather arbitrary way:

$$\sigma_{\text{total}}=\sigma_{\text{cantilever (single)}}+\Delta\sigma_{\text{tip (perturbation)}}.$$

The first distribution $\sigma_{\text{cantilever(single)}}$ is the same as that used in Sec. III B and consists in a continuous charge density all over the plane, including the area where tip is attached. The second distribution $\Delta\sigma_{\text{tip(perturbation)}}$ is a distribution of equivalent charges located on the z axis, that modifies the potential between the cantilever and the surface plane so as to make the shape of the equipotential V_0 fit the geometry of the real tip. This distribution is different from: $\sigma_{\text{tip(single)}}$; it includes negative charges (for positive V_0) near the plane of the cantilever that neutralize σ_{total} in the area where the tip is attached. The potential V and the force F are linear functions of σ, so we can write:

$$V_{\text{total}}=V_{\text{single cantilever}}+V_{\text{tip pertubation}}.$$

Thus the system that will give us the q_i' is:

$$\frac{1}{4\pi\epsilon_0}\sum_{i=1}^{N}\left(\frac{q_i'}{|\mathbf{r}_n-\mathbf{r}_1|}-\frac{q_i'}{|\mathbf{r}_n+\mathbf{r}_1|}\right)$$
$$=V_0(\mathbf{r}_n)-V(\mathbf{r}_n)_{\text{cantilever}}=\Delta V_{\text{tip perturbation}}. \quad (5)$$

The shape of equipotential obtained for a tip-cantilever system at the potential $V_0=1$ in front of a conductive plane at zero potential is represented in Fig. 8. The force can be expressed as a sum:

$$F_{\text{total}}=F_{\text{cantilever}}+\Delta F_{\text{tip}}$$
$$=F_{\text{cantilever}}+\frac{1}{4\pi\epsilon_0}\sum_{j=1}^{N}\sum_{i=1}^{N}\frac{-q_i'q_j'}{|\mathbf{r}_1+\mathbf{r}_j|^2}, \quad (6)$$

The dependence of the force versus d is shown in Fig. 7. We note that the environment of the cantilever is negligible inasmuch as the distances are small $d<10$ nm for tip A and $d<100$ nm for tip B. In all ranges, the force acting on the tip+cantilever system is very close to the sum of the two components calculated independently, which indicates that the calculation presented here is not always necessary.

To summarize, to obtain the real force on the whole sensor (tip+cantilever), we recommend the simple addition of the $F_{\text{cantilever}}$ force to the expressions given in Table I.

IV. DISCUSSION AND COMPARISON WITH THE EXPERIMENTS

The result of the previous section shows that, for distances larger than few nanometers, the cantilever plays a great part in the expression of electrostatic force especially for tips A. The experimental verification has been made with

an AFM. Park Scientific Instrument system. We used a silicon tip type A ($k=0.16$ N/m) and silicon nitride tip type B ($k=0.03$ N/m) covered with gold. In $F(d)$ force mode, the deflection of the cantilever is measured and the absolute value deduced after correct calibration of microscope. Figure 7 shows that the experimental points obtained in the air are correctly located on the theoretical curve and prove that the cantilever provides the bulk of the measured force for distances $d>10$ nm. In the air, we were not able to obtain experimental confirmation for smaller distances than those presented in Fig. 7 for two reasons: the water film on the plane creates a meniscus when $d<5$ nm, which force is much larger than the electrostatic forces. For tip B, the cantilever is very flexible and the static flexure is instable at distance of less than 15 nm.

The presence of the force on the cantilever induces several problems in the imagery of potentials for metal objects in air. When the electrostatic force due to the cantilever is important, the resolution of the microscope is reduced,[22] but a suitable choice of distance and tip shape can solve this problem.[9] In Fig. 7, our experimental result have shown that tip B gives large electrostatic force at $d=10$ nm, mainly localized on the apex, which may give a correct compromise between force and resolution values. Some authors have obtained the same result by shielding the tip.[23]

In the resonant mode, the relative effect of the cantilever is decreased because its force is nearly independent on the distance ($d<100$ nm), and acts as a constant force ignored by the feed-back in the noncontact mode.

V. CONCLUSION

We have developed a precise model (equivalent charge model) to calculate the electrostatic force acting on different types of tip in front of a plane surface for any distances. This model does not make any approximation concerning the shape of the tip and does not need arbitrary parameters. We have compared the exact values of the force with analytic models commonly used to approximate electrostatic forces. For short or medium tip sample distances, we have deduced that the spherical model and the uniformly charged line model, respectively, are good approximations of the true values. These two approximations correspond to the case of an electrostatic force localized on the apex or on the conical side of the tip.

We have shown that the force acting on the cantilever prevails for distances $d>10$ nm in the case of sharp and short tips ($R=10$ nm) and this result has been confirmed by experiments. This phenomenon can be partly corrected by taking tips with larger angles, apex radii or lengths.

Our next study concerns the comparison of the spatial resolution in the static mode and in the resonant mode, this last mode being supposedly less sensitive to the cantilever force and others static perturbations.

APPENDIX: ANALYTIC MODELS

The sphere model

The capacity of two spheres is deduced from the expression of the force between a sphere and a plane.[24]

$$F=2\pi\epsilon_0 V_0^2\sum_{n=1}^{\infty}\left(\frac{\coth\ \alpha-n\ \coth(n\alpha)}{\mathrm{sh}(n\alpha)}\right)$$

with

$$\alpha=\mathrm{argch}\left(\frac{d+R}{R}\right). \tag{A1}$$

In these case $d\ll R$, the force reduces to:

$$F\cong\pi\epsilon_0 V_0^2\frac{R}{d}. \tag{A2}$$

When the distance d is much larger than the length L of the tip, the sphere approximation may be again used. A convenient expression includes a $(L/2d)^2$ term which appears in the force acting on the sphere, and a coefficient $s(\theta)$ sensitive to the real shape of the tip:

$$F=\pi\epsilon_0 V_0^2\left(\frac{L}{2d}\,s(\theta)\right)^2. \tag{A3}$$

As the total charge of the tip obtained in the equivalent charge model seems approximately linear versus the half angle of the cone, we suggest a semi-empirical law in the force expression:

$$s(\theta)=a\theta+b \tag{A4}$$

$a=0.13$ and $b=0.72$ can be used in the $5<\theta<50°$ range.

The single charge model

A single charge in front of a plane produces a distribution of potential which approximates a sphere. This approximation is valid when the distance between the charge and the plane is much larger than the radius R of the sphere. For lower distances, this model can be used if we place the equivalent charge q at a distance such that the curvature of the equipotential V_0 is equal to R at the point closest to the plane (Fig. 9). The subsequent values of a and q can be determined easily from the equation of equipotentials in a dipole system, and for $d\ll R$ reduced to

$$a^2\cong 3Rd, \tag{A5}$$

$$q\cong 6\pi\epsilon_0 V_0 R, \tag{A6}$$

$$F=\frac{1}{4\pi\epsilon_0}\frac{q^2}{4a^2}\cong\frac{3}{4}\,\pi\epsilon_0 V_0^2\frac{R}{d}. \tag{A7}$$

The above force is close but not equal to the force for the spheric case because the spheroïdal equipotential created by a single charge is slightly different from that of a sphere (Fig. 9)

The knife edge model[18]

The knife edge model considers the tip as a thin edge of infinite length along the z axis and width l along the y

$$F=\frac{2V_0^2\epsilon_0}{\pi}\frac{l}{d}. \tag{A8}$$

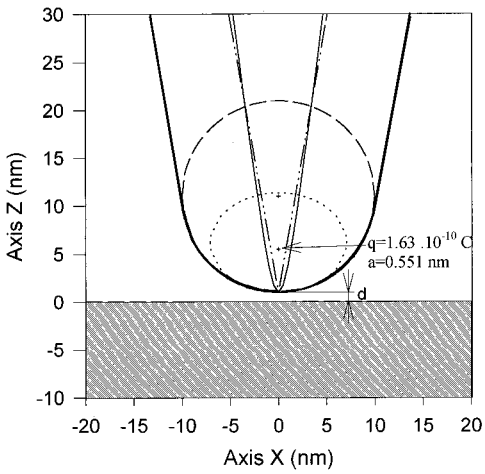

FIG. 9. Tip shape used in the different several analytic expressions used to calculate the electrostatic force for a tip A_1, — hyperbole with the asymptotes of equations $y=1/\tan(10°)x$, -- sphere of radius $R=10$ nm, ----- equipotentials of 1 V created by a single charge with the curvature of radius $R=10$ nm in $X=0$ and such as $(R/d)=10$, —- cone of opening $\theta=10°$, — real tip.

The perfect cone model

On the basis of the dimension equation, Yokoyama[25] foresees a logarithmic dependence of the force on the distance for an infinite cone in front of a plane. For a finite cone, an approximation for $d \ll D$ can be used:

$$F(d) \cong a \ln\left(\frac{D}{d}\right), \tag{A9}$$

where a and D are constant depending on the angle and the length of the cone.

The numerical simulation of the perfect cone with the equivalent charges model enables us to confirm the above expression and evaluate a and D; we thus obtain $a=1.954\times10^{-3}$ nN/V^2 and $D=10$ μm for the tip A_1.

The hyperboloid model[26]

The procedure uses the prolate spheroïdal coordinate transformation. The force is obtained by integrating the electrostatic pressure exercised on the plane by an infinite tip. As the total force applied by the hyperboloid is not finite, it seems correct to simulate a finite tip by integrating the force only on a circular area of the radius equal to the length of the tip. This approximation apply only if $d \ll L$.

The uniformly charged line model[17]

The model of the uniform charge distribution on a line gives equipotentials representative of the conical part of the probe. For a infinite, uniformly charged line of line density λ, the potential is given by the expression:

$$V(x,z) = \frac{\lambda}{4\pi\epsilon_0} \ln\left(\frac{z_1+z+\sqrt{(z_1+z)^2+x^2}}{z_1-z+\sqrt{(z_1+z)^2+x^2}}\right), \tag{A10}$$

where z_1 is the position of the lower extremity of the charged line on the z axis:

$$z_1 = d\sqrt{(1+\tan^2\theta)}.$$

An infinite cone with a half angle θ is obtained when

$$\lambda = \frac{2\pi\epsilon_0 V_0}{\mathrm{Argsh}(\tan^{-1}\theta)}. \tag{A11}$$

For instance, conical tips with 1 V potential and of $\theta_1=10°$ and $\theta_2=35°$ angles can be obtained with $\lambda_1=2.27\times10^{-11}$ C/m and $\lambda_2=4.81\times10^{-11}$ C/m, respectively. It should be noted that the force is not defined for tips of infinite length. The real length of the tip is introduced by taking only a charged segment of length L between z_1 and z_1+L. In this case, the force is given by:

$$F = \frac{\lambda^2}{4\pi\epsilon_0} \ln\left(\frac{(2z_1+L)^2}{4z_1(z_1+L)}\right), \tag{A12}$$

which for small distances ($d \ll L$) and small angles reduces to: $F=\lambda^2/4\pi\epsilon_0 \ln(L/4d)$. This expression is close to the expression for a perfect cone, the difference coming from the apex radius which is zero in a cone and finite in the charged line model.

The plane surface model[7]

This model approximates the tip-plane system to a plane capacitor system. The force is:

$$F = \frac{\epsilon_0 V_0^2}{2} \frac{A}{d^2}, \tag{A13}$$

where A represents the surface of a tip. If we take $A=\pi R^2$, we obtain the force on a tip with a broken end.

[1] G. Binning and H. Rohrer, Helv. Phys. Acta **55**, 726 (1982).
[2] Y. Martin, C. C. Williams, and H. K. Wrickramasinghe, J. Appl. Phys. **61**, 4723 (1987).
[3] G. Binning, C. F. Quate, and Ch. Gerber, Phys. Rev. Lett. **56**, 930 (1986).
[4] N. A. Burnham, R. J. Colton, and H. M. Pollock, J. Vac. Sci. Technol. A **9**, 2548 (1991).
[5] T. R. Albrecht and C. F. Quate, J. Appl. Phys. **62**, 2599 (1987).
[6] Y. Martin and H. K. Wrickramasinghe, Appl. Phys. Lett. **50**, 1455 (1987).
[7] Y. Martin, D. W. Abraham, and H. K. Wrickramasinghe, Appl. Phys. Lett. **52**, 1103 (1988).
[8] A. S. Hou, F. Ho, and D. M. Bloom, Electron. Lett. **28-25**, 2302 (1992).
[9] C. Böhm, F. Saurenbach, P. Taschner, C. Roths, and E. Kubalek, J. Phys. D **26**, 1801 (1993).
[10] S. R. A. Said, G. E. Bridges, and D. J. Thomson, Appl. Phys. Lett. **64**, 1442 (1994).
[11] S. Hudlet, M. Saint Jean, B. Roulet, J. Berger, and C. Guthmann, J. Appl. Phys. **77**, 3308 (1995).
[12] P. Girard, S. Belaidi, and G. Cohen-Solal, Microelectron. Eng. **31**, 215 (1996).
[13] Y. Liang, D. A. Bonnell, W. D. Goodhue, D. D. Rathman, and C. O. Bozler, Appl. Phys. Lett. **66**, 1147 (1995).
[14] S. Watanabe, K. Hane, M. Ito, and T. Goto, Appl. Phys. Lett. **63**, 2573 (1993).
[15] K. Domansky, Y. Leng, C. C. Williams, J. Janata, and D. Petelenz, Appl. Phys. Lett. **63**, 1513 (1993).
[16] B. D. Terris, J. E. Stern, D. Rugar, and H. J. Mamin, Phys. Rev. Lett. **63**, 2669 (1989).
[17] H. W. Hao, A. M. Baro, and J. J. Saenz, J. Vac. Sci. Technol. B **9**, 1323 (1991).
[18] C. Böhm, C. Roths, U. Müller, A. Beyer, and E. Kubalek, Beam Injection

Assessment of defects in Semiconductors (BIADS '93), Bologna, Italy, 1993.
[19] U. Müller, S. Hofschen, C. Böhm, J. Sprengepiel, E. Kubalek, and A. Beyer, 5th Electron and Optical Beam Testing Conference, Wuppertal, Germany, 1995, Microelectron. Eng. **31** (1996).
[20] S Watanabe, H. Kane, T. Ohye, M. Ito, and T. Goto, J. Vac. Sci. Technol. B **11**, 1774 (1993).
[21] U. Hartmann, R. Wiesendanger, and H. Güntherodt, in *Scanning Tunneling Microscopy III*, series in Surfaces Sciences (Springer, New York, 1993), Vol. 29, p. 293.
[22] T. Hochwitz, H. K. Henning, C. Leveg, C. Daghlian, and J. Slinkman, J. Vac. Sci. Technol. B **14**, 457 (1996).
[23] W. Nabhan, A. Broniatowski, G. de Rosny, and B. Equer, Microsc. Microanal. Microstruct. **5**, 237 (1994).
[24] E. Durand, *Electrostatique, Tome II Problèmes généraux, Conducteurs* (Masson &cie, 1966), p. 207.
[25] H. Yokoyama, T. Inoue, and J. Itoh, Appl. Phys. Lett. **65**, 3143 (1994).
[26] L. H. Pan, T. E. Sullivan, V. J. Peridier, P. H. Cutler, and N. M. Miskovsky, Appl. Phys. Lett. **65**, 2151 (1994).